Korean Journal of Remote Sensing, Vol.23, No.1, 2007, pp.7~14

Absolute Atmospheric Correction Procedure for the EO-1 Hyperion Data Using MODTRAN Code

Sun-Hwa Kim, Sung-Jin Kang, Jun-Hwa Chi, and Kyu-Sung Lee†

Department of Geoinformatic Engineering, Inha University

Abstract : Atmospheric correction is one of critical procedures to extract quantitative information related to biophysical variables from hyperspectral imagery. Most atmospheric correction algorithms developed for hyperspectral data have been based upon atmospheric radiative transfer (RT) codes, such as MODTRAN. Because of the difficulty in acquisition of atmospheric data at the time of image capture, the complexity of RT model, and large volume of hyperspectral data, atmospheric correction can be very difficult and time-consuming processing. In this study, we attempted to develop an efficient method for the atmospheric correction of EO-1 Hyperion data. This method uses the pre-calculated look-up-table (LUT) for fast and simple processing. The pre-calculated LUT was generated by successive running of MODTRAN model with several input parameters related to solar and sensor geometry, radiometric specification of sensor, and atmospheric condition. Atmospheric water vapour contents image was generated directly from a few absorption bands of Hyperion data themselves and used one of input parameters. This new atmospheric correction method was tested on the Hyperion data acquired on June 3, 2001 over Seoul area. Reflectance spectra of several known targets corresponded with the typical pattern of spectral reflectance on the atmospherically corrected Hyperion image, although further improvement to reduce sensor noise is necessary.

Key Words : Atmospheric correction, hyperspectral, Hyperion, water vapour contents, MODTRAN, reflectance.

1. Introduction

Hyperspectral data contain hundreds of continuous and narrow spectral bands and have great advantage in deriving complete spectral characteristics of surface materials (Goetz, 1991). In recent years, the use of hyperspectral data has continuously increased to extract biophysical information related to vegetation, rock, water, or military targets (Kim *et al.*, 2005; Miesch *et al.*, 2005). Since the first airborne imaging spectrometer, Airborne Imaging Spectrometer (AIS), in 1983, several airborne sensors such as AVIRIS and HyMap have been developed. The first and, probably, the only one civilian spaceborne hyperspectral sensor, the Hyperion has been operating on NASA's experimental satellite EO-1 launched in 2000 (Qu *et al.*, 2003; Kim *et al.*, 2005).

To derive complete spectral reflectance curve from

Received 21 December 2006; Accepted 12 February 2007.

† Corresponding Author: K. – S. Lee (ksung@inha.ac.kr)

hyperspectral imagery, atmospheric correction must be carried out to convert at-sensor radiance to surface reflectance (Richter and Schlapfer, 2002). Atmospheric correction of hyperspectral data is basically to remove atmospheric attenuations from the at-sensor radiance and to achieve accurate surface reflectance value, which can be analysed with various sources (i.e., spectral library) of known spectral characteristics of surface materials (Griffin and Burke, 2003; Qu *et al.*, 2003). Atmospheric correction of optical remote sensor data can be divided into two major category. Relative atmospheric correction is simple to apply and does not require atmospheric data. On the other hands, absolute atmospheric correction is based on physical process of radiative transfer and, therefore, very complex and requires a lot of information regarding sun-surface-sensor geometry, atmospheric condition at the time of data capture, and sensor's radiometric specifications (Cairns *et al.*, 2003). To calculate the physical process of radiation transfer from the earth's surface to sensor, most absolute atmospheric correction methods use radiative transfer (RT) model, such as MODTRAN and 6S (Richter and Schlapfer, 2002). Several atmospheric correction solutions based on such RT models have been developed for hyperspectral data and they are now available as in commercial product, such as ATREM, ACORN, FLAASH, and HATCH (Gao *et al.*, 1993; Richter and Schlapfer, 2002; Goetz *et al.*, 2003; Griffin and Burke, 2003).

Considering the large volume of hyperspectral data and complexity of running RT model, atmospheric correction method should be simple and fast for end users while it still maintain the accuracy. The accuracy of atmospheric correction greatly depends on the information related to atmospheric water vapour and aerosol at the time of image data acquisition (Cairns *et al.*, 2003). Fortunately, several algorithms were already developed to extract atmospheric information directly from hyperspectral data itself. The objective of this study is to develop relatively simple, fast, and accurate atmospheric correction algorithm for the Hyperion hyperspectral data. Currently, the Hyperion data are the only available hyperspectral image data over the Korean peninsula as well as many other parts of the world and this study intends to provide a simple way of implementing atmospheric correction to Hyperion data.

2. Methods

Figure 1 shows the overall procedure of the atmospheric correction algorithm for Hyperion hyperspectral data suggested in this study. For accurate and fast atmospheric correction of the hyperspectral image data, we attempt to generated site-specific water vapour contents data directly from hyperspectral image and the pre-calculated look-up-table (LUT). Water vapour content image is directly obtained from a few spectral bands of the hyperspectral data to be corrected.

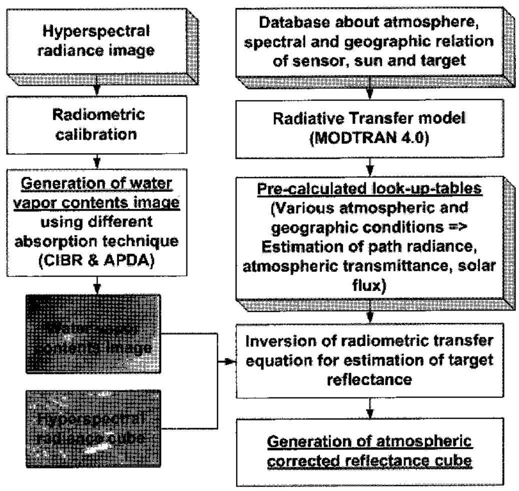

Figure 1. Overall procedure of absolute atmospheric correction for hyperspectral data.

Using the water vapour content information at the time of image data acquisition, atmospheric correction can be more reliable and, perhaps, more accurate. Instead of calculating the radiative transfer process for every pixel, we used a LUT approach for the fast calculation to convert at-sensor radiance to surface reflectance.

1) Generation of water vapour contents image data

Water vapour content is one of key components in atmospheric correction and absorber of solar radiation (Schlapfer *et al.*, 1998). The distribution and amount of water vapour at the time of image capture are important for atmospheric correction of optical imagery. Because of the difficulty in ground measurement of atmospheric constituents and the poor spatial resolution of meteorological satellite data, absolute atmospheric correction of high resolution satellite image has been challenging. Narrow-band hyperspectral image data contain several spectral absorption bands that allow us to estimate atmospheric gases and water vapour content. Since the development of hyperspectral data, several algorithms have been developed to estimate atmospheric water vapour content (Gao and Kaufman, 1990; Schlapfer *et al.*, 1998). In this study, we adopted two algorithms that were based on a strong atmospheric water absorption feature in near infrared spectrum: CIBR (continuum interpolated band ratio) and APDA (atmospheric pre-corrected differential absorption technique) methods. These algorithms are basically using the ratio between a water absorption band and nearby normal bands. As seen in Figure 2, both methods used the spectral reflectance values at three spectral bands of an absorption bands (940nm) and two non-absorption bands (842nm, 1300nm). The depth of spectral absorption feature at 940nm is proportional to the atmospheric water vapour content and can be determined from the local continuum that

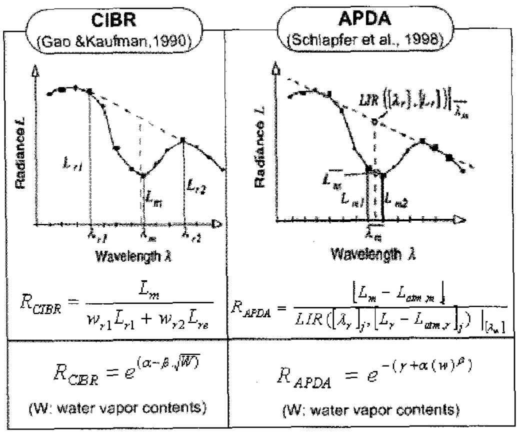

Figure 2. CIBR and APDA methods for estimating atmospheric water vapour contents.

connects two neighbouring non-absorption features at 842nm and 1300nm. Atmospheric water content was then estimated from the ratio value (R) for every pixel location.

2) Pre-calculation of look-up-table (LUT)

Atmospheric radiative transfer code is a rather complex numerical model and used to calculate atmospheric scattering and absorption and eventually to get surface reflectance. MODTRAN (MODerate resolution atmospheric radiance and TRANsmittance Model) has been a frequently used for atmospheric correction of satellite imagery. In this study, the inversion mode of MODTRAN model was used to acquire surface reflectance from at-sensor radiance. To calculate surface reflectance from at-sensor radiance, several input parameters are required, which includes atmospheric model, aerosol model, geometric information of sun-target-sensor, and sensor spectral specification. Because hyperspectral data have more than two hundreds spectral bands and atmospheric correction should be performed on every pixel, the atmospheric correction procedure should be fast. We tried to implement pre-calculated LUT that directly calculates transmittance, path radiance, and solar radiation on ground with several input parameters required in MODTRAN (Figure 3). LUT are composed of the calculated atmospheric effects (path radiance, transmittance and radiation flux) for every combination of pre-defined values for several input parameters (Table 1), which include atmospheric parameters, solar and sensor geometry, sensor spectral wavelength and response function. The first sequence of obtaining LUT is to calculate path radiance, transmittance, and global flux value for every input parameter combination for the Hyperion data. Using these information, the surface reflectance is ultimately calculated using these LUT values at next stage.

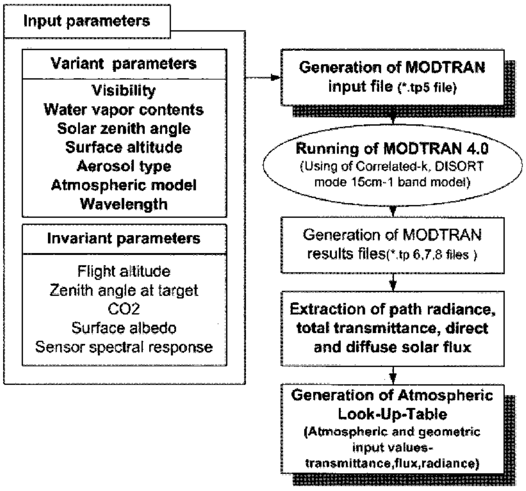

Figure 3. Flow chart to generate pre-calculated LUT.

Table 1. Pre-defined input parameters for MODTRAN to generate the LUT.

Variant input parameters			
Parameters	Range	Interval	Values
Water vapour contents	0.5-4.0 gcm-2	0.5	0.5, 1.0, 1.5, 2.0, 2.5, 3.0, 3.5, 4.0
Aerosol type	Rural, Urban	-	Rural, Urban
Atmosphere model	Mid-latitude summer, winter	-	Mid-latitude summer, winter
Visibility	5-120km	5km/ 20km	5, 10, 15, 20, 30, 40, 60, 80, 100, 120
Surface altitude	0-2.5km	0.5km	0, 0.5, 1.0, 1.5, 2.0, 2.5
Solar zenith angle	0-70°	10°	0, 10, 20, 30, 40, 50, 60, 70
Spectral bands	400-2500nm	10nm	-
Invariant input parameters			
Flight altitude CO2 Surface albedo Sensor spectral response			705km 365ppm 0.135 Hyperion

3) Conversion of at-sensor radiance to surface reflectance

The radiance value (L) received on-board sensor can be expressed in a simple form of equation (Eq. 1) and can be easily obtained by applying the known calibration coefficients to pixel's digital number (DN) value of the hyperspectral image. Three unknown terms in the right side of the equation are path radiance (Lp), atmospheric transmittance (τ), and radiation flux on the ground (Eg). These three components are obtained from the LUT, which were pre-calculated using MODTRAN with several input parameters of atmospheric and geometric conditions. The surface reflectance value (ρ) is then calculated by the inversion of the equation 1. The inversion processing is applied to every spectral band and every pixel of hyperspectral data.

$$L(\lambda) = L_p(\lambda) + \tau(\lambda)\rho(\lambda)E_g(\lambda)/\pi \quad \text{(Eq. 1)}$$

$L(\lambda)$: Sensor-received radiance for each channel λ

$Lp(\lambda)$: Path radiance

$\tau(\lambda)$: Atmospheric transmittance

$\rho(\lambda)$: Surface reflectance

$Eg(\lambda)$: radiation flux on the ground

3. Experiments

1) Study area and data used

To apply and validate the atmospheric correction algorithm, we used EO-1 Hyperion data acquired on

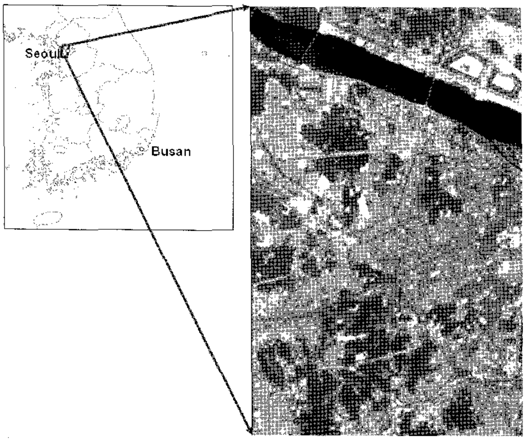

Figure 4. The Hyperion image showing the study area in western part of Seoul.

Table 2. Specification of the Hyperion data used in this study.

Items	Specifications
Sensor	EO-1 Hyperion
Date	June 3, 2001 A.M. 11:02
Image size	400 R * 256 C
Spectral band	242 bands (400 - 2,500 nm)
Band width	10 nm
Spatial resolution	30 m × 30 m
Solar zenith angle	24.42°

June 3, 2001 over Seoul area (Figure 4). Hyperion data is satellite-borne hyperspectral data and has 242 spectral bands ranging from approximately 400 to 2,500nm. Table 2 shows the specification of Hyperion data used in this study. Study area covers about 9,200ha, located near Han river of the western Seoul, and includes several cover types of urban, road, forest, grass, and water body.

2) Atmospheric correction results

In absolute atmospheric correction of hyperspectral data, the atmospheric water content should be extracted for every pixel location using a few spectral bands of the hyperspectral data. Figure 5 shows the water vapour contents images that were generated by the two estimation methods (CIBR and APDA). Both

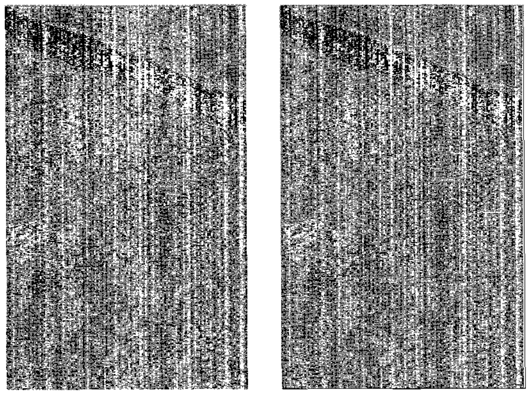

Figure 5. Water vapour content images generated by using CIBR (left) and APDA (right) algorithms from the Hyperion data over the study area.

Table 3. Statistics of water vapour contents estimates.

(unit: cm)

Statistics	CIBR	APDA
Min-Max	0.19 - 4.13	0.21 - 3.80
Mean	2.22	1.80
Std	0.52	0.44

images look very similar and show vertical strip that is clear indication of sensor noise. The images also show no distinct variation by land cover types. Water vapour content per atmospheric column with the CIBR method provides a little higher values (Table 3). Although it is not possible to verify which method would provide the actual atmospheric condition because of the difficulty of obtaining the exact ground truth, we used the water vapour content image estimated by the APDA method. The APDA method is known to be less sensitive to surface reflectance and provide better estimate of atmospheric water content (Schlapfer *et al.*, 1998).

Figure 6 shows atmospheric transmittance values extracted from the pre-calculated LUT for various water vapour contents. Transmittance value at water absorption band (942nm) is decreased as atmospheric water vapour content increases. On the other hands, transmittance values at non-absorption bands (842nm, 1003nm) are more or less constant

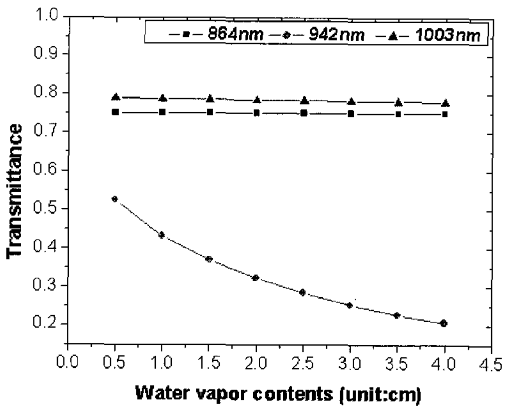

Figure 6. Transmittance values extracted from the pre-calculated LUT for various water vapour contents at an water absorption band (942nm) and non-absorption bands (864nm, 1003nm).

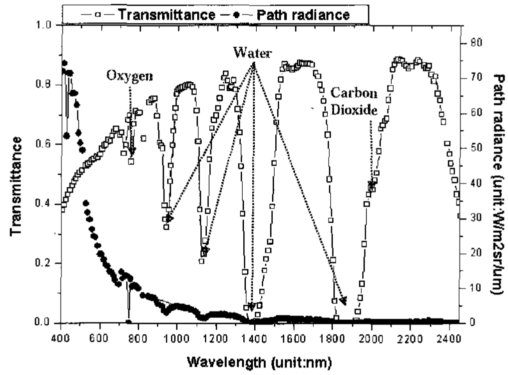

Figure 7. Transmittance and path radiance obtained from the pre-calculated LUT (water vapour contents=2.0cm, visibility= urban 15km, surface altitude=0.5km).

regardless of atmospheric water vapour contents.

The pre-calculated LUT was further evaluated under various atmospheric conditions. Figure 7 showed transmittance and path radiance extracted from the pre-calculated LUT at specific atmospheric condition. As well known, the high atmospheric scattering in blue wavelength region contributes such large values of path radiance. The pre-calculated LUT also clearly demonstrates several absorption features caused by atmospheric water vapour and gases in the estimated transmittance curve.

The pre-calculated LUT instantly depicts atmospheric transmittance, path radiance, and radiation flux on ground when we provide the input parameters related to atmospheric data, sun and sensor geometry, and sensor's spectral response function. Among these input parameters, atmospheric water content and elevation, derived from digital elevation model data, vary for every pixel while the other input parameters are spatially homogeneous for a whole scene of hyperspectral image. Although we used standard types of atmospheric and aerosol models that come with MODTRAN code, further refinement of the LUT is possible with the ones that are more appropriate to local condition at the time of image capture. The use of the pre-calculated LUT accelerates processing speed because it can avoid operating the MODTRAN code for every pixel.

Once the pre-calculated LUT was developed, the Hyperion radiance image, water vapour image, and other input parameters were assembled to derive surface reflectance. In our program to process the whole sequence of the atmospheric correction, it took about four minutes to obtain atmospherically corrected surface reflectance image of the study area. Figure 8 shows spectral reflectance curves of several ground features extracted from the atmospherically

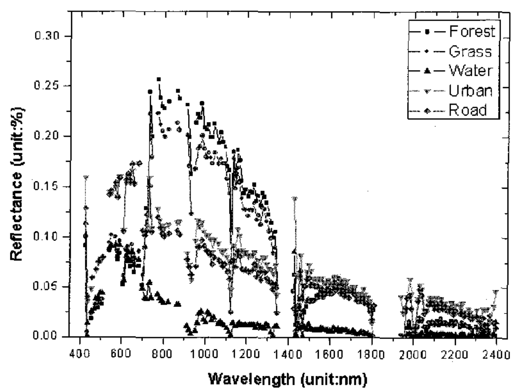

Figure 8. Spectral reflectance curves of various ground features, which were extracted from the atmospherically corrected Hyperion data over the study area.

corrected Hyperion reflectance image. Although the reflectance values in near infrared (NIR) wavelength (700 - 1,300nm) seems to be a little low, forest and grass show the distinctive pattern of green vegetation in which the high reflectance at NIR region and low reflectance in visible wavelength. Water body has very low reflectance values over visible region and is almost no reflectance beyond near infrared region. Spectral patterns of urban and road are very similar each other. Although these spectra acceptably agree with the typical form of spectral reflectance, they show some noises that may come from the Hyperion sensor itself. Further more, it is essential to have accurate data for those input parameters related to the atmospheric condition at the time of hyperspectral data acquisition. In this study, except for the atmospheric water vapour content, we just used standard form of atmospheric data that comes with MODTRAN code. In particular, exact information regarding the spatial distribution of aerosol density can be an important input parameter to achieve more accurate atmospheric correction of the hyperspectral data.

4. Conclusions

Atmospheric correction is an essential procedure to extract accurate reflectance spectra from hyperspectral data, it is often difficult and time-consuming. In this study, we developed an atmospheric correction procedure that can be simple and fast to implement. For accurate atmospheric correction, we initially generated atmospheric water vapour contents image using different absorption algorithm from hyperspectral data itself and used it in subsequent atmospheric correction procedure.

In this atmospheric correction method, we developed the pre-calculated LUT that was obtained from MODTRAN code. The pre-calculated LUT provides transmittance, path radiance, and solar radiation flux, under specific sets of various input parameters including atmospheric data, solar and sensor geometry, and sensor spectral response function. Atmospherically corrected surface reflectance is then obtained from hyperspectral radiance data by using three components (transmittance, path radiance, and solar radiation flux) derived the LUT. Use of the pre-calculated LUT was very effective in time and process for the atmospheric correction of more than two hundreds bands of the hyperspectral data. Although the Hyperion reflectance value obtained by this atmospheric correction method seems little lower, the spectral reflectance curves of several surface materials relatively well corresponds with typical pattern. Further refinement of the LUT using more reliable atmospheric data and the pre-processing technique to reduce the inherent sensor noise of Hyperion imaging spectrometer should improve the atmospheric correction effects.

Acknowledgements

This research was supported by the Agency for Defense Development, Korea, through the Image Information Research Center at Korea Advanced Institute of Science & Technology.

References

Cairns, B., B. E. Carlson, R. Ying, A. A. Lacis, and V. Oinas, 2003. Atmospheric correction and its application to an analysis of Hyperion data. *IEEE Transactions on Geoscience and Remote Sensing*, 41(6): 1232-1244.

Gao, B. and Kaufman Y. J., 1990. Column atmospheric water vapour and vegetation liquid water retrievals from airborne imaging spectrometer data. *Journal of geophysical research*, 95(4): 3549-3564.

Gao, B., Heidebrecht K. B., and Goetz A. F. H., 1993. Derivation of scaled surface reflectances from AVIRIS data. *Remote Sensing of Environment*, 44: 165-178.

Goetz, A. F. H., 1991. Imaging spectrometry for studying Earth, Air, Fire and Water. *EARSeL Advances in Remote Sensing*, 1: 3-15.

Goetz, A. F. H., B. C. Kinde, M. Ferri, and Z. Qu, 2003. HATCH: Results from simulated radiances, AVIRIS and Hyperion. *IEEE Transactions on Geoscience and Remote Sensing*, 41(6): 1215-1222.

Griffin, M. K. and H. K. Burke, 2003. Compensation of hyperspectral data for atmospheric effects. *Lincoln Laboratory Journal*, 14(1): 29-54.

Kim, S. H., K. S. Lee, J. R. Ma, and M. J. Kook, 2005. Current status of hyperspectral remote sensing: Principle, Data processing techniques, and Application. *Korean Journal of Remote Sensing*, 21(4): 341-369.

Miesh, C., L. Poutier, V. Achard, X. Briottet, X. Lenot, and Y. Boucher, 2005. Direct and inverse radiative transfer solutions for visible and near-infrared hyperspectral imagery. *IEEE Transactions on Geoscience and Remote Sensing*, 43(7): 1552-1562.

Qu, Z., B. C. Kindel, and A. F. H. Goetz, 2003. The High-Accuracy Atmospheric Correction for Hyperspectral data (HATCH) model. *IEEE Transactions on Geoscience and Remote Sensing*, 41(6): 1223-1231.

Richter, R. and D. Schlapfer, 2002. Geo-atmospheric processing of airborne imaging spectrometry data. Part 2: atmospheric/topographic correction. *International Journal of Remote Sensing*, 23(13): 2631-2649.

Schlapfer, D., C. C. Borel, J. Keller, and K. I. Itten, 1998. Atmospheric precorrected differential absorption technique to retrieve column water vapour. *Remote Sensing of Environment*, 65: 353-366.